

# New heterobimetallic Cu(II)/Mn(II) complexes with trans-1,8-cyclam derivatives: Synthesis, characterization, magnetic properties and crystal structures of ( $\mu_2$ -Chloro)-(dpc)-copper(II)-trichloro-manganese(II) and two polymorphs of ( $\mu_2$ -Chloro)-(dac)-copper(II)-trichloro-manganese(II)



Erika Samořová<sup>a</sup>, Juraj Kuchár<sup>b,\*</sup>, Erik Čiřmár<sup>c</sup>, Michal Duřek<sup>a</sup>

<sup>a</sup> Institute of Physics, Academy of Sciences of the Czech Republic, Cukrovarnická 10, Praha 16253, Czech Republic

<sup>b</sup> Department of Inorganic Chemistry, Pavol Jozef Šafárik University in Kořice, Moyzesova 11, Kořice 04154, Slovak Republic

<sup>c</sup> Department of Condensed Matter Physics, Pavol Jozef Šafárik University in Kořice, Park Angelinum 9, Kořice 04154, Slovak Republic

## ARTICLE INFO

### Article history:

Received 2 February 2021

Revised 28 April 2021

Accepted 29 April 2021

Available online 5 May 2021

### Keywords:

Heterobimetallic complexes

Cyclam derivatives

Crystal structure

Magnetic properties

## ABSTRACT

Two derivatives of cyclam (cyclam = 1,4,8,11-tetraazacyclotetradecane) with propyl- or allyl- (prop-2-en-1-yl) substituents on nitrogen atoms in trans positions, namely 1,8-dipropyl-1,4,8,11-tetraazacyclotetradecane (dpc) and 1,8-diallyl-1,4,8,11-tetraazacyclotetradecane (dac) were prepared and characterized by IR, <sup>1</sup>H NMR and <sup>13</sup>C NMR spectroscopy. Reaction of dpc and dac with copper(II) chloride gives compounds [Cu(dpc)(H<sub>2</sub>O)<sub>2</sub>Cl<sub>2</sub>] (1) and [Cu(dac)(H<sub>2</sub>O)<sub>2</sub>Cl<sub>2</sub>] (3) with similar crystal structures. Compounds 1 and 3 were used as precursors in the synthesis of Cu(II)/Mn(II) complexes 2, 4a and 4b. Prepared complexes were characterized by IR spectroscopy, elemental analysis and their crystal structures were determined using single crystal X-ray analysis. Compounds 4a and 4b are polymorphs, both crystallize in the monoclinic crystal system and the main difference in their crystal structures is in steric arrangement of metal centres within a chain. Moreover, measurements of magnetic susceptibility and Broken Symmetry DFT calculations (BS DFT calculations) carried out for bimetallic complexes 2 and 4a showed that a ferromagnetic exchange interaction  $J/k_B = 2.28$  K and  $J/k_B = 2.34$  K, respectively, exists within the dinuclear units.

© 2021 Elsevier B.V. All rights reserved.

## 1. Introduction

Magnetic phenomena associated with thermal effects have recently become relevant not only for solving fundamental problems in magnetism and solid-state physics but also for technological applications [1]. One such phenomenon is the magnetocaloric effect that can be used in the thermal study of magnetic properties of compounds, or for practical use, for example in magnetic refrigerators [2,3]. There are several ferrimagnetic complexes in which the magnetocaloric effect was observed [4,5]. It was predicted by Kahn et al. that systems based on one-dimensional bimetallic chains with alternating Cu(II) and Mn(II) atoms participating in antiferromagnetic (AFM) exchange interaction should show ferrimagnetic behavior [6,7] and this prediction has been confirmed in many complexes [8–10]. The ground state of ferrimagnetic chains

is of ferromagnetic (FM) nature with non-zero spontaneous magnetization. However, excitations are of AFM type [11] leading to the formation of magnetization plateaus and a large change of the magnetic entropy at the field-induced quantum-critical points [12].

For synthetic chemists, the targeted synthesis of coordination polymers remains the challenge for the last decades. We are interested in synthesis, characterization, and the study of magnetic properties of complexes with a 1D structure based on Cu(II) coordinated by N-donor ligands in equatorial positions and {MnCl<sub>4</sub>} particle. The key step in their synthesis is the selection of ligands, as they significantly influence the formation of chains and their arrangement in the crystal structure. Previously, we prepared series of complexes with Cu(II) atom coordinated by N-derivatives of ethane-1,2-diamine (Samořová, private commns.) in equatorial positions and chloride ligands in axial positions, the latter mediating the connection with Mn(II) atom that becomes tetracoordinated by chlorido ligands. Such an arrangement allows the formation of bimetallic chains with short chloride-bridged

\* Corresponding author.

E-mail address: [juraj.kuchar@upjs.sk](mailto:juraj.kuchar@upjs.sk) (J. Kuchár).

paramagnetic metals. For the preparation of this class of complexes, we choose the complex-as-ligand strategy, where Cu(II) complexes with *N*-donor ligands are prepared in the first step and then used in the reaction with Mn(II) chloride.

In this paper, we focused on the preparation and characterization of analogous compounds using macrocyclic ligands based on cyclam in the copper(II) coordination sphere. It is well known that copper(II) forms with this class of ligands complexes with appreciable kinetic and thermodynamic stability. This makes them convenient for the use of complex-as-ligand strategy by the preparation of bimetallic complexes. Although compounds **2** and **4a** can be regarded as chain-like alternating-spin systems, the major exchange interaction mediated by covalent bonds in Cu(II)-Mn(II) units is FM as suggested by our magnetic measurements and Broken Symmetry (BS) DFT calculations.

## 2. Experimental

### 2.1. Materials and physical measurements

All reagents and solvents except ligands *dac* and *dpc* were purchased from commercial sources and used without further purification. Infrared spectra were recorded on a Nicolet 6700 FT-IR spectrometer using ATR technique in the range of 4000–400 cm<sup>-1</sup>. Elemental analyses (C, H, N) were performed on a CHNS Elemental Analyzer VarioMICRO by Elementar Analysensysteme GmbH. <sup>13</sup>C NMR spectra of *dac* and *dpc* were obtained on a Bruker Ascent 400 spectrometer. Chemical shifts are given in ppm using tetramethylsilane as a standard.

Susceptibility (estimated as the ratio of measured magnetic moment and applied magnetic field) and magnetization was measured on a commercial Quantum Design MPMS3 magnetometer in the temperature range from 1.8 to 300 K at 100 mT. A nascent polycrystalline specimen was fixed in a gelatine capsule and the capsule was held by a straw. The signal contribution of the gelatine capsule and the diamagnetic contribution of the sample (estimated using Pascal's constants [13]) were subtracted.

### 2.2. Synthesis and crystallization

#### Ligands *dac* and *dpc*

The organic ligands *dac* and *dpc* were prepared according to the synthetic procedure (Scheme 1) described previously by Royal et al. [14]. 2 g of cyclam (99% purity, Merck) were dissolved in 100 ml of distilled water, and the solution was cooled to 0 °C with continuous stirring. 3.24 ml of formaldehyde (20 % molar excess, Merck, 37% solution in H<sub>2</sub>O) was rapidly added, and the stirring continued for 2 h. Formed white precipitate was filtered and dried at 60 °C. The dry precipitate was dissolved in acetonitrile, and 3 equiv. of 3-bromopropene (99% purity, Merck,) or 1-bromopropane (99% purity, Merck,) were rapidly added with continuous stirring. The reaction mixture was stirred 2 h for 3-bromopropene and 2 days in the case of 1-bromopropane, formed colourless precipitate was filtered, washed with acetonitrile and dried on air. 1 g of prepared compound 1,8-dipropyl-4,11-diazoniatricyclo[9.3.1.14,8]-hexadecane dibromide or 1,8-diallyl-4,11-diazoniatricyclo[9.3.1.14,8]-hexadecane

dibromide was dissolved in 250 ml 3M NaOH and stirred for 3 h, consequently extracted with CH<sub>2</sub>Cl<sub>2</sub>, the extract was dried with anhydrous MgSO<sub>4</sub>, filtered and the solvent was removed by distillation under vacuum. Ligands *dac* and *dbc* prepared using this method were characterized by IR spectroscopy, <sup>1</sup>H and <sup>13</sup>C NMR spectroscopy.

#### *dac*

<sup>1</sup>H NMR (400 MHz, CDCl<sub>3</sub>) δ 5.87 (tdd, *J* = 23.7, 10.3, 6.7 Hz, 2H, CH<sub>2</sub>=CH-), 5.21 – 5.16 (m, 2H, CH<sub>2</sub>=CH-), 5.16 – 5.14 (m, *J* = 2.3 Hz, 2H, CH<sub>2</sub>=CH-), 3.16 (s, 2H, NH), 3.12 (d, *J* = 6.7 Hz, 4H, CH<sub>2</sub>=CH-CH<sub>2</sub>), 2.73 – 2.63 (m, 8H, α-CH<sub>2</sub>), 2.57 – 2.49 (m, 8H, α-CH<sub>2</sub>), 1.80 – 1.73 (m, 4H, β-CH<sub>2</sub>)

<sup>13</sup>C NMR (101 MHz, CDCl<sub>3</sub>) δ = 134.72 (CH<sub>2</sub>=CH-), 117.99 (CH<sub>2</sub>=CH-), 56.64 (α-CH<sub>2</sub>), 53.61

(α-CH<sub>2</sub>), 53.07 (α-CH<sub>2</sub>), 50.55 (α-CH<sub>2</sub>), 47.70 (α-CH<sub>2</sub>), 25.78 (β-CH<sub>2</sub>)

IR: ν(NH) 3297 (w), ν(=C-H) 3073 (vw), ν(CH) 2921 (m), 2800 (m), ν(C=C) 1643 (w), δ(CH<sub>2</sub>) 1458 (m), 1332 (m), ν(CN) 1130 (m), ω(CH<sub>2</sub>) 913 (s)

Yield: 1.3 g (52%)

#### *dpc*

<sup>1</sup>H NMR (400 MHz, CDCl<sub>3</sub>) δ 3.35 (s, 2H, NH), 2.75 – 2.60 (m, 8H, α-CH<sub>2</sub>), 2.55 – 2.45 (m, 8H, α-CH<sub>2</sub>), 2.43 – 2.36 (m, 4H, -CH<sub>2</sub>-CH<sub>2</sub>-CH<sub>3</sub>), 1.79 – 1.71 (m, 4H, β-CH<sub>2</sub>), 1.49 (dq, *J* = 14.8, 7.4 Hz, 4H, -CH<sub>2</sub>-CH<sub>2</sub>-CH<sub>3</sub>), 0.86 (t, 6H, -CH<sub>3</sub>).

<sup>13</sup>C NMR (101 MHz, CDCl<sub>3</sub>) δ = 53.76 (α-CH<sub>2</sub>), 51.82 (α-CH<sub>2</sub>), 51.38 (α-CH<sub>2</sub>), 48.56 (α-CH<sub>2</sub>), 46.62 (α-CH<sub>2</sub>), 29.27 (-CH<sub>2</sub>-CH<sub>3</sub>), 22.95 (β-CH<sub>2</sub>), 11.86 (CH<sub>3</sub>)

IR: ν(NH) 3279 (vw), ν(CH) 2957 (w), 2931 (w), 2873 (w) 2805(m), δ(CH<sub>2</sub>) 1459 (m), 1381 (w), ν(CN) 1164 (m), ω(CH<sub>2</sub>) 744(s)

Yield: 1g (31.5%)

#### Synthesis of [Cu(*dpc*)(H<sub>2</sub>O)<sub>2</sub>]Cl<sub>2</sub> (**1**)

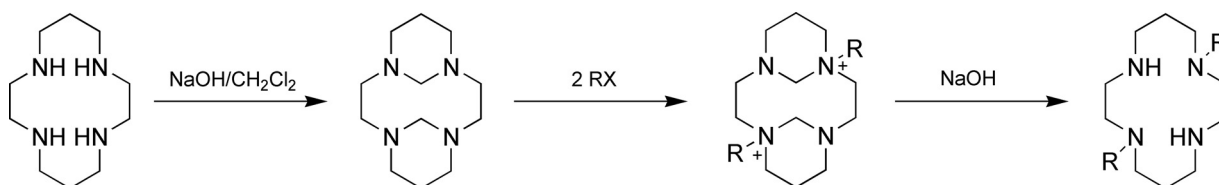
0.8 g of *dpc* (2.81 mmol) were dissolved in 70 ml of ethanol and heated to 65 °C. The solution of 0.48 g CuCl<sub>2</sub>·2H<sub>2</sub>O (2.81 mmol, p.a., Merck) in 20 ml of ethanol was added slowly, and the resulting solution was stirred at the same temperature for one hour, then filtered and the solution was allowed to crystallize at room temperature. In two weeks dark-violet crystals of **1** were formed and collected by filtration.

CHN (calc./exp.): C: 42.24/42.43; H: 8.86/8.35; N: 12.31/12.57

IR: ν(OH) 3442 (w), ν(NH) 3176 (m), 3131(m), ν(CH) 2958 (m), 2878 (m), δ(OH<sub>2</sub>) 1636 (w), δ(NH) 1474 (m), 1463 (m), δ(CH<sub>2</sub>) 1426 (m), 1390 (w), ν(CN) 1104 (m)

#### Synthesis of Cu(*dpc*)MnCl<sub>4</sub> (**2**)

0.27 g (0.59 mmol) of **1** was dissolved in 40 ml of ethanol and heated to 65 °C. The solution of 0.12 g MnCl<sub>2</sub>·4H<sub>2</sub>O (0.59 mmol, p.a., Merck) in 10 ml of ethanol was slowly added, and the resulting solution was refluxed for 3 h. The formed violet precipitate was filtered hot and dried on air. Dark red crystals of **2** were obtained within one week by recrystallization of precipitate from ethanol using diffusion of acetone vapor. The crystalline product was used for measurements of magnetic susceptibility and magnetization.



Scheme 1. Synthetic route for the ligand synthesis.

**Table 1**  
Crystal data and results of the refinement.

	1	2	3	4a	4b
Crystal data					
Chemical formula	C <sub>16</sub> H <sub>40</sub> Cl <sub>2</sub> Cu N <sub>4</sub> O <sub>2</sub>	C <sub>16</sub> H <sub>36</sub> Cl <sub>4</sub> Cu MnN <sub>4</sub>	C <sub>16</sub> H <sub>36</sub> Cl <sub>2</sub> Cu N <sub>4</sub> O <sub>2</sub>	C <sub>16</sub> H <sub>32</sub> Cl <sub>4</sub> Cu MnN <sub>4</sub>	C <sub>16</sub> H <sub>32</sub> Cl <sub>4</sub> Cu MnN <sub>4</sub>
M <sub>r</sub>	455	544.8	450.9	540.8	540.8
Crystal system, space group	Triclinic, P-1	Monoclinic, P2 <sub>1</sub> /n	Triclinic, P-1	Monoclinic, P2 <sub>1</sub> /n	Monoclinic, P2 <sub>1</sub> /c
Temperature (K)	150	95	170	120	170
a, b, c (Å)	7.9494 (6), 8.5551 (6), 8.6372 (4)	9.2800 (2), 17.4845 (3), 14.6176 (3)	7.7409 (4), 8.4657 (4), 8.8343 (3)	9.3198 (3), 16.7006 (4), 14.4346 (6)	14.7060 (3), 19.3297 (5), 16.3937 (4)
α, β, γ (°)	92.055 (5), 106.840 (5), 110.813 (6)	90, 102.110 (2), 90	93.819 (3), 106.905 (4), 111.114 (4)	90, 94.162 (3), 90	90, 94.854 (2), 90
V (Å <sup>3</sup> )	519.16 (7)	2319.02 (8)	507.12 (5)	2240.75 (13)	4643.40 (19)
Z	1	4	1	4	8
Radiation type	Mo Kα	Cu Kα	Mo Kα	Cu Kα	Mo Kα
μ (mm <sup>-1</sup> )	1.33	9.86	1.36	10.21	1.93
Crystal size (mm)	0.24 × 0.12 × 0.09	0.47 × 0.09 × 0.04	0.22 × 0.16 × 0.09	0.32 × 0.07 × 0.05	0.23 × 0.17 × 0.07
Data collection					
Diffractionmeter	SuperNova, Dual, Cu at home/near, AtlasS2	SuperNova, Dual, Cu at home/near, AtlasS2	Xcalibur, Sapphire2, large Be window	Xcalibur, AtlasS2, Gemini ultra	Xcalibur, Sapphire2, large Be window
Absorption correction	Multi-scan [15]	Multi-scan [15]	Multi-scan [15]	Multi-scan [15]	Analytical numeric absorption correction [19].
Tmin, Tmax	0.925, 1	0.32, 1	0.883, 1	0.412, 1	0.761, 0.916
No. of measured, independent and observed [I > 3σ(I)] reflections	9105, 2598, 2331	38010, 4686, 4343	11247, 2514, 2002	23492, 3123, 2833	24618, 9627, 5839
R <sub>int</sub>	0.022	0.043	0.031	0.063	0.037
(sin θ/λ) <sub>max</sub> (Å <sup>-1</sup> )	0.698	0.624	0.690	0.600	0.692
Refinement					
R[F <sup>2</sup> > 2σ(F <sup>2</sup> )], wR(F <sup>2</sup> ), S	0.023, 0.061, 1.59	0.024, 0.060, 1.61	0.028, 0.062, 1.37	0.030, 0.075, 1.94	0.039, 0.091, 1.31
No. of reflections	2598	4686	2514	3123	9627
No. of parameters	124	241	124	243	481
No. of restraints	3	2	3	2	4
ρ <sub>max</sub> , ρ <sub>min</sub> (e·Å <sup>-3</sup> )	0.31, -0.23	0.49, -0.43	0.37, -0.34	0.42, -0.39	0.82, -0.88

CHN (calc/exp.): C: 35.28/34.59; H: 6.66/6.48; N: 10.28/9.99  
 IR: ν(NH) 3184 (w), 3160 (m), ν(CH) 2961 (m), 2941 (m), 2877 (m), δ(NH) 1475 (m), 1469 (m), δ(CH<sub>2</sub>) 1428 (m), 1384 (w), ν(CN) 1102 (m)

#### Synthesis of [Cu(dac)(H<sub>2</sub>O)<sub>2</sub>]Cl<sub>2</sub> (**3**)

1.2 g of dac (4.28 mmol) was dissolved in 70 ml of ethanol and heated to 65 °C. The solution of 0.73 g CuCl<sub>2</sub>·2H<sub>2</sub>O (4.28 mmol, p.a., Merck) in 20 ml of ethanol was added slowly, and the resulting solution was stirred at the same temperature for one hour, then formed violet precipitate was filtered and the solution was al-

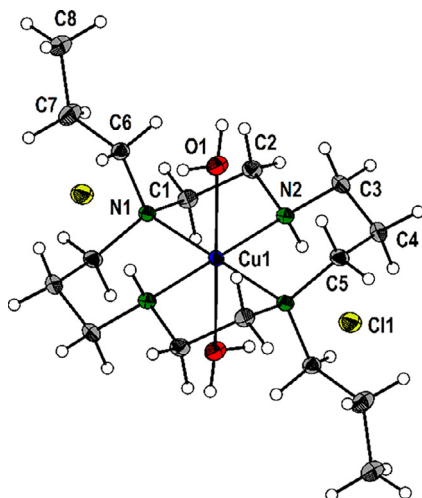


**Fig. 1.** The structure motif in **1**. Thermal ellipsoids are drawn on the 50 % probability level.

lowed to crystallize at room temperature. Within one week, dark-violet crystals of **3** were formed and collected by filtration.

CHN (calc/exp.): C: 42.62/42.81; H: 8.05/8.13; N: 12.42/12.37  
 IR: ν(OH) 3323 (w), ν(NH) 3183 (w), ν(CH) 3095 (w), 2916 (s), 2848 (s), ν(C=C) 1638 (w), δ(OH<sub>2</sub>) 1611 (w), δ(CH<sub>2</sub>) 1463 (s), 1421 (m), ν(CN) 1064 (m)

#### Synthesis of Cu(dac)MnCl<sub>4</sub> (**4a**)

0.5 g of **3** (1.11 mmol) was dissolved in 100 ml of ethanol and heated to 65 °C. The solution of 0.22 g MnCl<sub>2</sub>·4H<sub>2</sub>O (1.11 mmol, p.a., Merck) in 10 ml of ethanol was slowly added, and the resulting solution was refluxed for 3 h. The formed violet precipitate was

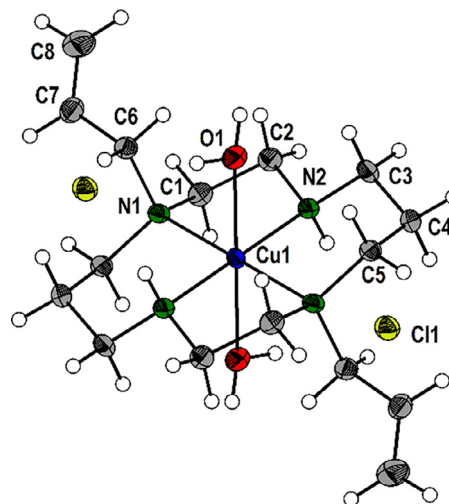


**Fig. 2.** The structure motif in **3**. Thermal ellipsoids are drawn on the 50 % probability level.

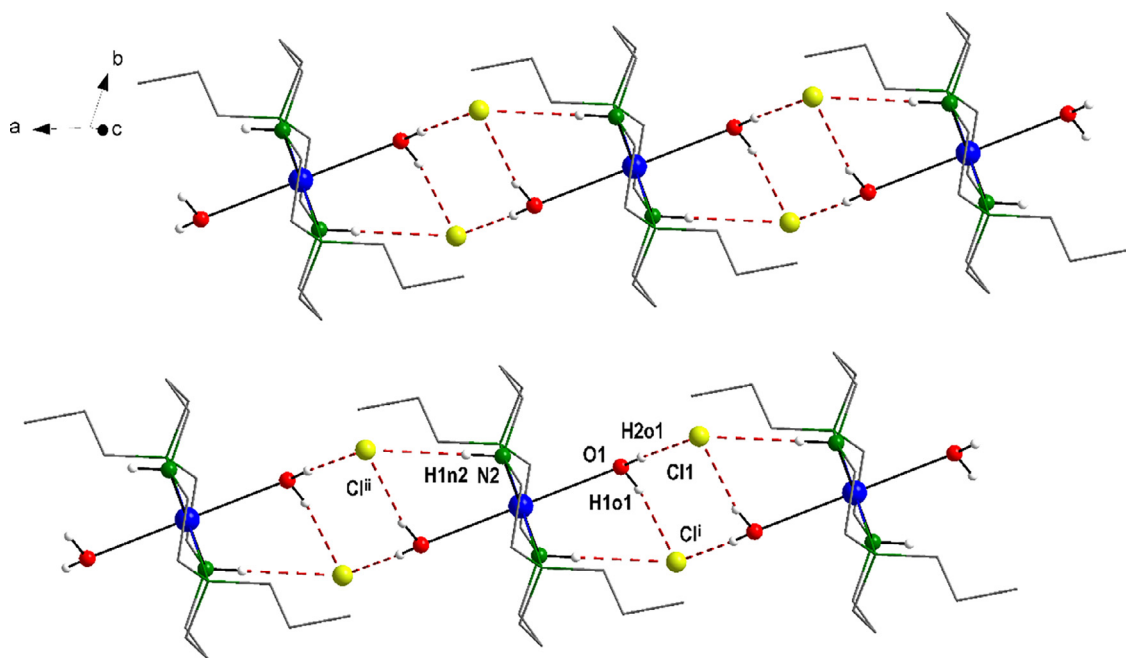


Fig. 3. Schematic view of the hydrogen bond system in **1**. i: 1-x, 1-y, 1-z; ii: 1+x, y, z.

filtered hot and dried on air. Dark red crystals of **4a** were obtained within one week by recrystallization of precipitate from ethanol using diffusion of acetonitrile vapor. The crystalline product was used for measurements of magnetic susceptibility and magnetization.

CHN (calc/exp): C: 35,54/35,3; H: 5,96/5,99; N: 10,36/10,14

IR:  $\nu(\text{NH})$  3170 (w), 3153 (m),  $\nu(\text{CH})$  2976 (w), 2951 (w), 2917 (w), 2873 (w),  $\nu(\text{C}=\text{C})$  1636 (w),  $\delta(\text{CH}_2)$  1469 (m), 1456 (m), 1427 (m), 1417 (w),  $\nu(\text{CN})$  1099 (m)

Synthesis of  $\text{Cu}(\text{dac})\text{MnCl}_4$  (**4b**)

0.255 g (0.61 mmol) of **3** was dissolved in ethanol (50 ml),  $\text{MnCl}_2 \cdot 4\text{H}_2\text{O}$  (0.12 g, 0.61 mmol, p.a., Merck) was added, and the resulting solution was heated under reflux for 3 h, then filtered hot and allowed to crystallize at room temperature. Within one week red crystals of **4b** were formed and collected by filtration.

CHN (calc./exp): C: 35.29/34.94; H: 5.92/6.02; N: 10.29/10.03

Table 2

Geometrical parameters characterizing coordination sphere of Cu(II) atom in **1** and **3**.

	<b>1</b>	<b>3</b>
Cu1-N1	2.1051(10)	2.0049(14)
Cu1-N2	1.9981(12)	2.0092(14)
Cu1-O1	2.5647(14)	2.5676(18)
N1-Cu1-N2	86.77(4)	86.24(6)
O1-Cu1-N1	95.37(6)	87.255(6)
O1-Cu1-N2	93.20(6)	84.049(6)

Table 3

Hydrogen bonding parameters in **1** and **3**.

	D-H...A	D-H	H...A	D...A	D-H...A
<b>1</b>	O1-H1O1...Cl1 <sup>i</sup>	0.849(16)	2.343(15)	3.1825(12)	169.6(17)
	N2-H1N2...Cl1 <sup>ii</sup>	0.870(11)	2.432(11)	3.2979(16)	173.3(12)
	O1-H2O1...Cl1	0.850(14)	2.300(14)	3.1488(12)	177.1(14)
i: 1-x, 1-y, 1-z; ii: 1+x, y, z					
<b>3</b>	O1-H1O1...Cl1 <sup>i</sup>	0.850(19)	2.321(18)	3.1597(16)	169.1(19)
	O1-H2O1...Cl1 <sup>ii</sup>	0.850(16)	2.323(16)	3.1711(15)	176.2(15)
	N2-H1N2...Cl1	0.870(14)	2.444(14)	3.3092(18)	173.1(17)
i: 1-x, -y, 1-z; ii: x-1, y, z					

IR:  $\nu(\text{NH})$  3136 (w),  $\nu(\text{CH})$  2941 (w), 2878 (w),  $\nu(\text{C}=\text{C})$  1640 (vw),  $\delta(\text{CH}_2)$  1460 (m), 1429 (m),  $\nu(\text{CN})$  1101 (m)

### 2.3. Refinement

Single crystal experiments were carried out on a four-circle  $\kappa$  axis Xcalibur2 diffractometer equipped with a CCD detector Sapphire 2 (Rigaku OD) using  $\text{MoK}\alpha$  radiation for **3** and **4b**, four-circle diffractometer Supernova (Rigaku OD) equipped with a CCD detector Atlas S2 using  $\text{CuK}\alpha$  for **1** and **2**, and four-circle diffractometer Gemini using  $\text{CuK}\alpha$  radiation for **4a**. Because the measurements were undertaken with different chillers allowing for different optimal lowest temperatures, the data were acquired at different temperatures, which is nevertheless acceptable due to the absence of phase transition effects. The CrysAlisPro [15] software was used for data collection, reduction, and correction for absorp-

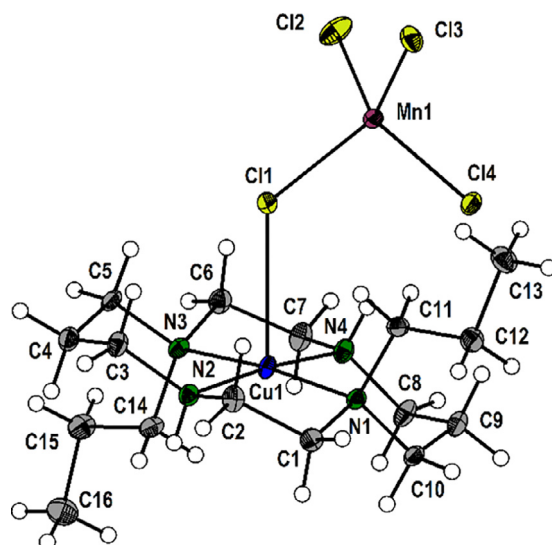


Fig. 4. The bimetallic complex in **2**. Thermal ellipsoids are drawn on the 50 % probability level.

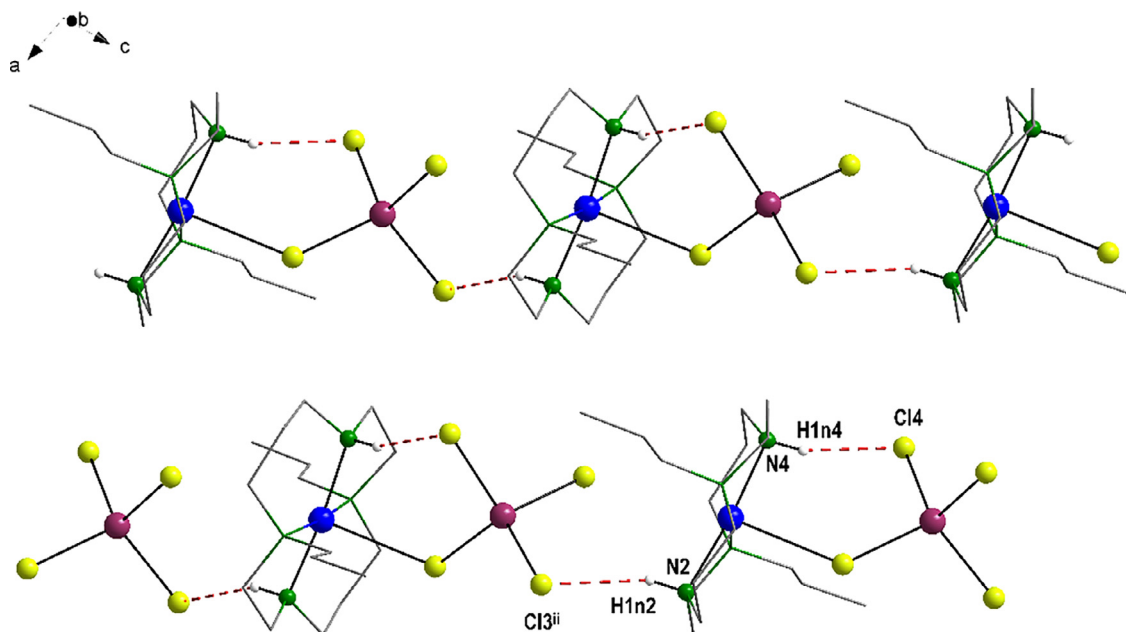


Fig. 5. Hydrogen bonds in the crystal structure of **2**. ii:  $\frac{1}{2}+x, \frac{1}{2}-y, -\frac{1}{2}+z$ .

tion for all compounds. In all cases, the model was found using Superflip [16]. An anisotropic refinement by full-matrix least-squares was performed with JANA2006 [17]. Non-hydrogen atoms were refined with anisotropic ADPs, and the hydrogen atoms on carbon atoms were placed at calculated positions refined on parent atoms. Hydrogens of nitrogen atoms and water molecules were found in a difference Fourier map and refined in the riding mode using bond restraint 0.87 Å for N-H and 0.85 Å for O-H, with s.u. of both restraints being 0.001. Crystal data and parameters of the structure refinement for all compounds are summarized in Table 1. The figures of structures were drawn using the DIAMOND software [18]. In the case of **4a**, the crystals were twinned, and for structure refinement, the reflections of a stronger domain and twinning matrix were used. Using the twinning matrix, differences in theta between reflections of both domains were calculated and sorted to the following shells: 0.0–0.1 - fully overlapped reflections, 0.1–0.3 - no reflections, 0.3–0.4–870 partially overlapped reflections (out of 3993 independent reflections), 0.4–0.6 - no reflections. Discarding the 870 partially overlapped reflections improved *R*, *GOF*, and

the overall values of atomic displacement parameter (ADP). Experimental details: H atoms were treated by a mixture of independent and constrained refinement.

#### 2.4. Computational details

The BS DFT calculation [20] was performed using the ORCA 4.0.1 computational package [21]. The calculation was done using the PBE0 exchange-correlation functional [22]. The zeroth-order regular approximation (ZORA) [23,24] together with the scalar relativistic contracted version of basis functions Def2-TZVP(-f) [25] was used. The calculations utilized the RI approximation and the chain-of-spheres (RIJCOSX) approximation to exact exchange [26] with appropriate decontracted auxiliary basis sets [27,28]. Increased integration grids (Grid4 and GridX4) and tight SCF convergence criteria were used. The exchange coupling was obtained using the Yamaguchi formalism [29]  $J_{BS} = -\frac{E_{HS} - E_{BS}}{S_{HS}^2 - S_{BS}^2}$  from single-point approach (using X-ray determined structure),

Table 4

Geometrical parameters characterizing coordination sphere of central atoms Cu(II) and Mn(II) in **2**.

Cu1-N1	2.1049(13)	N1-Cu1-N2	87.04(5)
Cu1-N2	1.9998(14)	N1-Cu1-N3	174.09(6)
Cu1-N3	2.0784(13)	N2-Cu1-N3	92.82(5)
Cu1-N4	1.9943(13)	N3-Cu1-N4	86.33(5)
Cu1-Cl1	2.8341(1)	Cl1-Mn1-Cl4	105.962(18)
Mn1-Cl1	2.3907(5)	Cl1-Mn1-Cl3	108.435(16)
Mn1-Cl2	2.3478(6)	Cl1-Mn1-Cl2	112.729(18)
Mn1-Cl3	2.3588(5)	Cl4-Mn1-Cl3	116.979(16)
Mn1-Cl4	2.3721(4)	Cl4-Mn1-Cl2	106.527(17)
N2-Cu1-N4	174.17(6)	Cl3-Mn1-Cl2	106.38(2)
N1-Cu1-N4	93.21(5)	Cu1-Cl1-Mn1	121.628(1)

Table 5

Hydrogen bonding parameters in **2**.

D-H...A	D-H	H...A	D...A	D-H...A
N2-H1N2...Cl1 <sup>ii</sup>	0.870(14)	2.724(19)	3.4999(16)	149.2(15)
N4-H1N4...Cl4	0.870(16)	2.490(19)	3.3189(16)	159.5(15)

ii:  $1/2+x, 1/2-y, z-1/2$

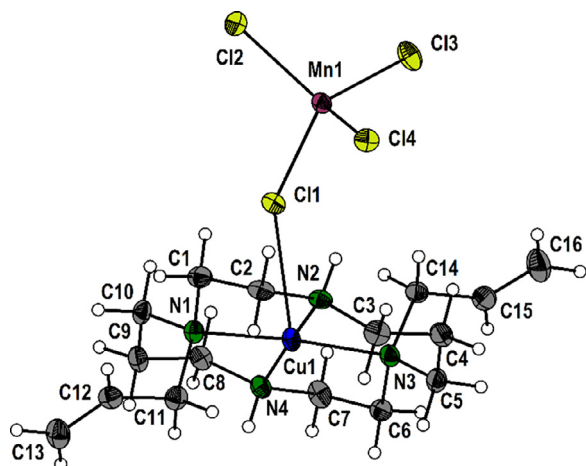


Fig. 6. The complex molecule in **4a**. Thermal ellipsoids are drawn on the 50 % probability level.

with a spin Hamiltonian in the form  $\mathcal{H} = -2J_{BS}\hat{S}_1\hat{S}_2$  (in the comparison with the experimental data a spin Hamiltonian in the form  $\mathcal{H} = -J\hat{S}_1\hat{S}_2$  was used).

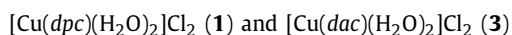
### 3. Results and discussion

Reaction of *dpc* and *dac* with copper(II) chloride gives compounds  $[\text{Cu}(\text{dpc})(\text{H}_2\text{O})_2]\text{Cl}_2$  (**1**) and  $[\text{Cu}(\text{dac})(\text{H}_2\text{O})_2]\text{Cl}_2$  (**3**), namely diaqua-((1,8-dipropyl-1,4,8,11-tetraazacyclotetradecane- $\kappa^4\text{N}$ )-copper(II) chloride) and diaqua-((1,8-diallyl-1,4,8,11-tetraazacyclotetradecane- $\kappa^4\text{N}$ )-copper(II) chloride), with similar crystal structures. Compounds **1** and **3** were used as precursors in the synthesis of Cu(II)/Mn(II) complexes, ( $\mu_2$ -Chloro)(1,8-dipropyl-1,4,8,11-tetraazacyclotetradecane- $\kappa^4\text{N}$ )-copper(II)-trichlorido-manganese(II) (**2**) and two polymorphs of ( $\mu_2$ -Chloro)-(1,8-diallyl-1,4,8,11-tetraazacyclotetradecane- $\kappa^4\text{N}$ )-copper(II)-trichlorido-manganese(II) (**4a** and **4b**) differ in steric arrangement of metal centres within a chain.

#### 3.1. Synthesis

The strategy used for preparing bimetallic complexes can be considered as building blocks synthesis and was carried out using a slightly modified synthetic procedure published earlier [30]. In the first step, the ligand *dpc* or *dac* was added to the ethanolic solution of  $\text{CuCl}_2$ , and crystallization from the resulting solution gave compound **1** or **3**. Both were characterized and used as starting material in the second step of the synthesis, in which ethanolic solution of  $\text{MnCl}_2$  was added to the solution of copper(II) complex in the same solvent, and the resulting solution was heated under reflux for 3 h. For crystallization, two strategies were chosen: slow evaporation of the solvent under standard conditions, and diffusion of acetone vapour into the reaction mixture at the same temperature. For the synthesis starting from **1**, both crystallization strategies lead to the preparation of the same product **2**, but in the case of the synthesis starting from **3**, two polymorphs of  $[\text{Cu}(\text{dac})\text{MnCl}_4]$  were obtained, **4a** by diffusion technique and **4b** by slow evaporation of the solvent.

#### 3.2. Crystal structures



Compounds **1** and **3** have a similar crystal structure that consists of isolated Cu(II) complexes and uncoordinated chloride anions. The shape of Cu(II) coordination polyhedron is tetragonal bipyramidal with elongation in axial positions due to the Jahn-Teller effect. Two axial positions are occupied by the oxygen atoms

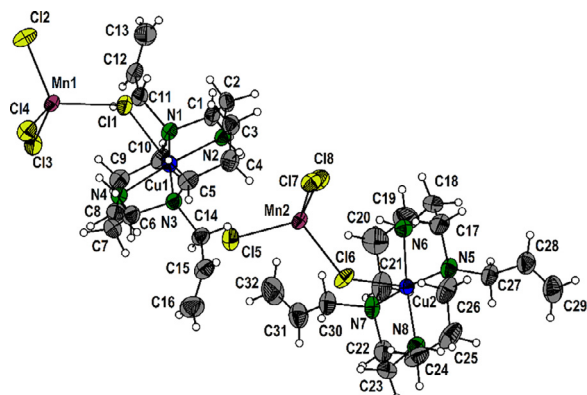
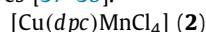


Fig. 7. The complex molecule in **4b**. Thermal ellipsoids are drawn on the 50 % probability level.

of water molecules and the basal ones by the nitrogen atoms from macrocyclic ligand *dpc* or *dac* (Figs. 1, 2). Cu-O distances are 2.5647(14) Å in **1** and 2.5685(17) Å in **3**, and they are comparable to distances in complexes with similar structure motif registered in CCDC with *cyclam* (2.535 Å) [31] or its derivatives (2.569 Å, 2.67 Å) [32,33]. In both cases, the coordinated macrocycle is in the *trans*-III configuration, which is usually the most stable configuration for such type of metal complexes [34]. Geometric parameters characterizing the coordination polyhedrons in both complexes are summarized in Table 2. In the crystal structure of **1** and **3**, aqua ligands, chloride anions, and amine groups of macrocycles participate in the hydrogen bond system including the O-H...Cl and N-H...Cl hydrogen bonds with moderate strength, considered due to the D-A distance length, angles values, and calculated hydrogen bond energies [35]. Two ring patterns can be described for the hydrogen bond system:  $R_2^1(6)$  including Cu(II) atom, one amine group of ligand, chloride anion, oxygen atom and one hydrogen atom from water molecule, and  $R_2^2(8)$  including two coordinated water molecules and two chloride anions [36]. The connections of complexes through the hydrogen bond system propagate in *a* direction. Schematic representation of hydrogen bonds in **1** is shown in Fig. 3, and geometrical parameters for both compounds can be found in Table 3. The described hydrogen bond system has been already observed in other copper(II) complexes with *cyclam* derivatives [37–39].



The structure of **2** consists of binuclear complexes where Mn(II) and Cu(II) ions are bridged by chlorido ligand. The steric arrangement of chlorido ligands in Mn(II) coordination environment is

Table 6  
Geometrical parameters characterizing coordination sphere of central atoms Cu(II) and Mn(II) in **4a** and **4b**.

<b>4a</b>		<b>4b</b>		
Cu1-N1	2.064(3)	2.075(3)	Cu2-N5	2.048(3)
Cu1-N2	1.992(3)	1.997(3)	Cu2-N6	1.987(4)
Cu1-N3	2.082(3)	2.052(3)	Cu2-N7	2.071(3)
Cu1-N4	1.999(3)	1.999(3)	Cu2-N8	1.989(3)
Cu1-Cl1	2.9453(9)	2.8631(12)	Cu2-Cl6	2.7988(12)
Mn1-Cl1	2.3909(9)	2.3834(12)	Mn2-Cl5	2.3431(12)
Mn1-Cl2	2.3488(10)	2.3482(13)	Mn2-Cl6	2.3815(12)
Mn1-Cl3	2.3383(9)	2.3660(11)	Mn2-Cl7	2.3669(11)
Mn1-Cl4	2.3844(8)	2.3651(12)	Mn2-Cl8	2.3657(12)
N2-Cu1-N4	175.34(11)	174.46(14)	N5-Cu2-N7	170.46(14)
N1-Cu1-N4	92.75(11)	93.68(13)	N5-Cu2-N6	86.09(14)
N1-Cu1-N2	86.03(11)	86.84(13)	N5-Cu2-N8	92.27(13)
N1-Cu1-N3	175.23(11)	172.72(13)	N7-Cu2-N6	94.65(14)
N2-Cu1-N3	94.21(11)	92.58(13)	N7-Cu2-N8	85.83(13)
N3-Cu1-N4	86.63(11)	86.20(13)	N6-Cu2-N8	172.86(15)
Cl1-Mn1-Cl4	103.84(3)	107.13(4)	Cl7-Mn2-Cl8	108.47(4)
Cl1-Mn1-Cl3	114.41(3)	106.41(4)	Cl7-Mn2-Cl6	109.16(4)
Cl1-Mn1-Cl2	109.72(3)	113.91(4)	Cl7-Mn2-Cl5	108.83(5)
Cl4-Mn1-Cl3	108.30(3)	111.27(4)	Cl8-Mn2-Cl6	105.99(5)
Cl4-Mn1-Cl2	108.09(3)	110.27(5)	Cl8-Mn2-Cl5	111.20(4)
Cl3-Mn1-Cl2	111.99(4)	107.83(4)	Cl6-Mn2-Cl5	113.06(4)
Cu1-Cl1-Mn1	123.632(4)	120.24(3)	Cu2-Cl6-Mn2	122.48(3)

Table 7  
Hydrogen bonding parameters in **4a** and **4b**.

	D-H...A	D-H	H...A	D...A	D-H...A
<b>4a</b>	N2-H1N2...Cl4	0.870(3)	2.44(3)	3.272(3)	158.89(3)
	N4 <sup>i</sup> -H1N4 <sup>i</sup> ...Cl4	0.870(3)	2.53(3)	3.282(3)	144.85(3)
i: 3/2-x, y-1/2, 1/2-z					
<b>4b</b>	N2-H1N2...Cl7	0.870(15)	2.485(15)	3.294(4)	155(3)
	N4-H1N4...Cl3	0.87(2)	2.429(19)	3.277(4)	165(3)
	N6-H1N6...Cl8	0.870(11)	2.423(14)	3.267(4)	164(4)
	N8-H1N8...Cl4 <sup>ii</sup>	0.870(15)	2.560(18)	3.323(4)	147(3)
ii: x, y-1, z					

close to tetrahedral, an average value of Mn-Cl bond distances is 2.367(16) Å, and the main deviation of tetrahedral symmetry is represented by the angle Cl4-Mn1-Cl3 with value 116.979(16)°. Cu(II) atom is pentacoordinated, the axial position is occupied by bridging chlorido ligand and four equatorial positions are occupied by nitrogen atoms of *dpc* ligand. Similar to compounds **1** and **3**, the bridging ligand is in *trans*-III configuration (Fig. 4). Cu(II) is placed 0.1046(3) Å above the plane defined by four nitrogen atoms (Table 4). In the crystal structure, both hydrogen atoms on nitrogen atoms participate in N-H...Cl hydrogen bonds, one of them being intramolecular and the second one connecting the nearest complex molecule. Thus, the connection between complex molecules propagates in *c* direction, the Cu-Cl distance between complexes in this direction is 3.5959(1) Å. Schematic representation of hydrogen bonds in **2** is shown in Fig. 5, and geometrical parameters can be found in Table 5.

#### [Cu(*dac*)MnCl<sub>4</sub>] (**4a**) and [Cu(*dac*)MnCl<sub>4</sub>] (**4b**)

The structure of both complexes contains the same complex molecule, analogous to **2** with *dac* ligand instead of *dpc*. In **4a** there is one crystallographically independent complex (Fig. 6) while **4b** contains two independent complex molecules (Fig. 7). The steric arrangement of chlorido ligands in Mn(II) coordination environment is close to tetrahedral in all cases, with an average Mn-Cl bond distance 2.37(2) Å for **4a**, 2.366(12) and 2.364(13) Å for Mn1 and Mn2 of **4b**. The main deviation of tetrahedral symmetry is represented by the angle Cl4-Mn1-Cl1 of 103.84(3)° in **4a**, and angles Cl2-Mn1-Cl1 of 113.91(4)° and Cl6-Mn2-Cl5 of 113.06(4)° in

**4b**. The Cu1-Cl1 distance in **4a** of 2.9453(9) Å is close to the sum of Van der Waals radii. In **4b** both Cu-Cl distances are slightly shorter, Cu1-Cl1 2.8628(11) Å and Cu2-Cl6 2.7987(11) Å. Similar to **2**, Cu(II) is placed slightly above the plane defined by nitrogen atoms from *dac*, with the distance from the plane 0.0825(4) Å for **4a**, and 0.1141(5) Å and 0.1471(5) Å for Cu1 and Cu2 of **4b** (Table 6). In both compounds, the complexes are connected by N-H...Cl hydrogen bonds and analogous to **2** the interaction propagates in one direction. The main difference between compounds **4a** and **4b** is the steric arrangement of complexes within hydrogen-bonded chains. In **4a** the Mn(II) atoms are placed above and under the line constructed through Cu(II) atoms approximately in *b* direction, whereas in **4b** the metal atoms are relatively in one line in *b* direction. In **4a** one chlorido ligand acts as an acceptor in two hydrogen bonds, one intramolecular and the second one intermolecular, in **4b** the situation is analogous to **2** and two chlorido ligands participate in hydrogen bonding (Table 7). The shortest Cu-Cl distance between complexes in **4a** has similar values as in the case of **2**, Cu1-Cl2 is 3.5271(9) Å, while in **4b** the corresponding distances are longer, Cu1-Cl5 is 3.8077(13) Å and Cu2-Cl2 3.8945(13) Å.

### 3.3. Magnetic properties

Our aim to synthesize ferrimagnetic systems with interesting behavior of magnetocaloric effect at elevated magnetic fields at low temperatures predicted by theory [12] led us to the detailed study of magnetic properties of **2** and **4a**. As the structure of both

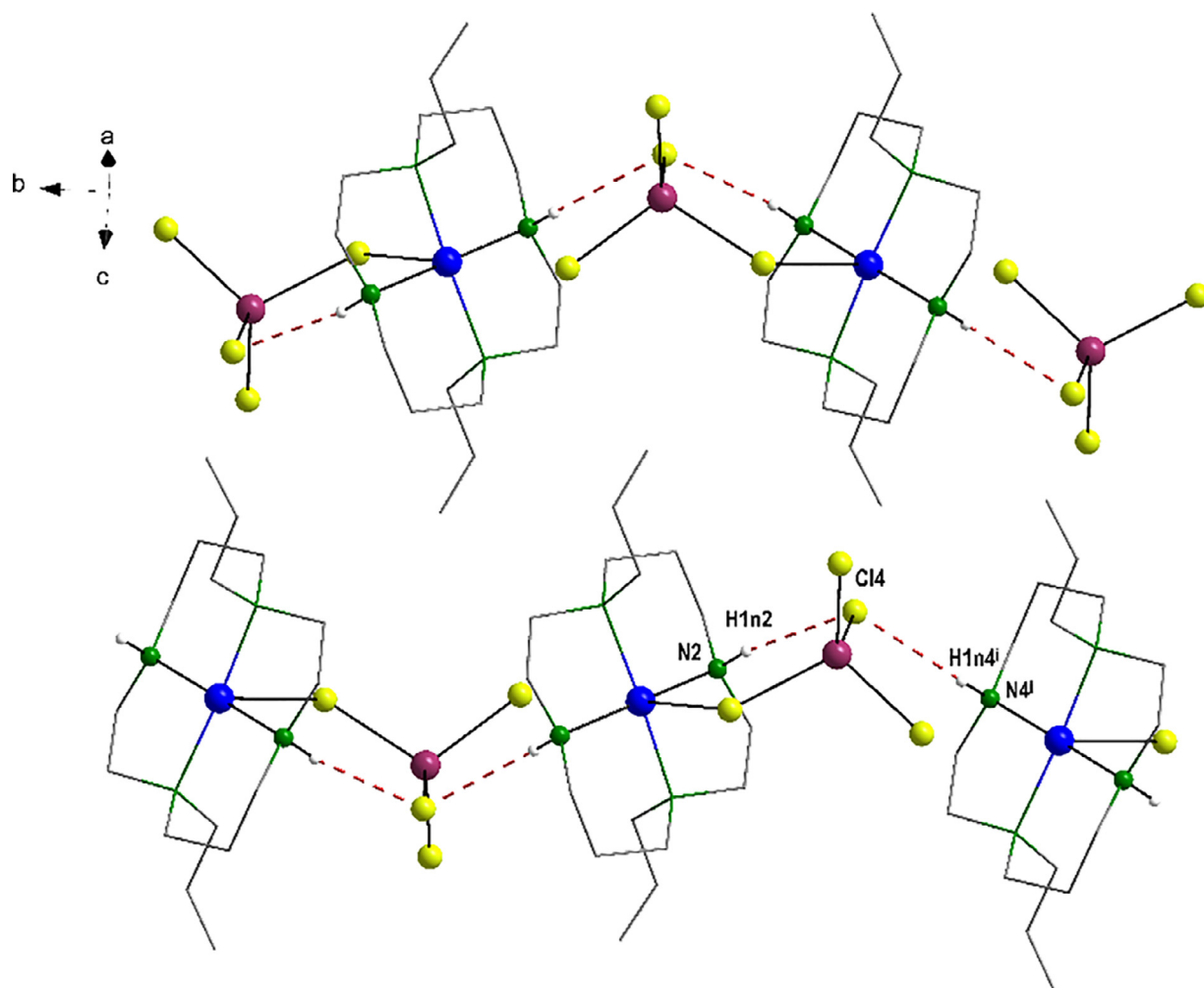


Fig. 8. Hydrogen bonds in the crystal structure of **4a**. i: 3/2-x, y-1/2, 1/2-z.

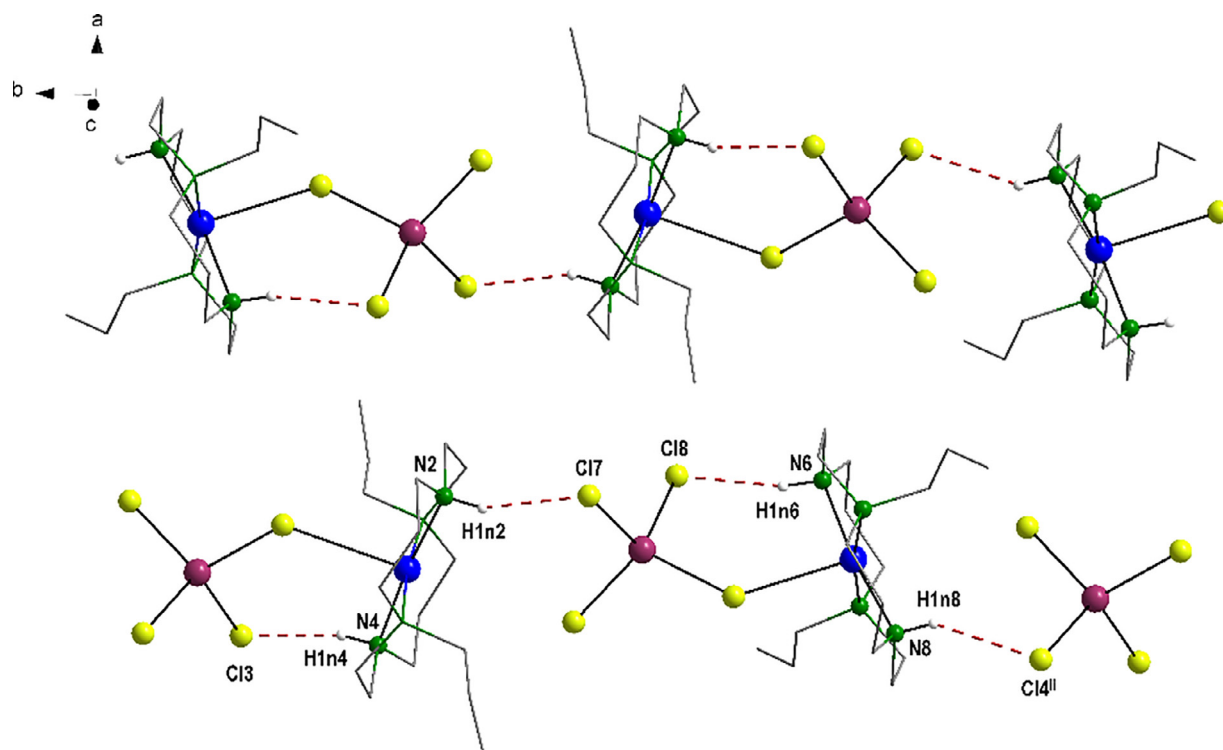


Fig. 9. Hydrogen bonds in the crystal structure of **4b**. ii: x, y-1, z.

compounds is formed by heteronuclear covalent dimeric units, the presence of AFM interaction could also suggest a possibility to study the quantum entanglement effects [40]. The room-temperature value of the effective magnetic moment of **2** and **4a**,  $\mu_{\text{eff}} = 6.23 \mu_{\text{B}}$  ( $\mu_{\text{B}}$  is Bohr magneton), is very close to the expected value  $\mu_{\text{eff}} = 6.2 \mu_{\text{B}}$  when Cu(II) ( $3d^9$ , spin  $S_{\text{Cu}} = 1/2$ ) and Mn(II) ( $3d^5$ , spin  $S_{\text{Mn}} = 5/2$ ) ions are present in the molecular unit in the paramagnetic limit (calculated using typical average values of  $g$ -factor 2.15 and 2.0 for Cu(II) and Mn(II) ions, respectively). While the temperature dependence of  $\chi T$  product of compound **4a** in Fig. 10 displays an increase below 50 K down to 10 K, the  $\chi T$  product of compound **2** shown in Fig. 11 is almost constant above 10 K. A sudden decrease of  $\chi T$  was observed below 10 K for both compounds. An indication of long-range magnetic order (LRO) was observed below 3.2 K in **2** as a difference between zero-field cooled (ZFC) and field cooled (FC) magnetic response (inset of Fig. 11).

Compounds **2, 4a**, and **4b**, may be regarded as chain-like spin systems (Figs. 5, 8, and 9) with the possibility to form interesting ferrimagnetic chains, in this case with alternating exchange interaction due to the alternation of covalent and hydrogen bonds between Cu(II) and Mn(II) ions in the chain. The susceptibility of ferrimagnetic chains (also with alternating bonds) is characterized by a decrease of  $\chi T$  with the decreasing temperature reaching a minimum followed by an increase of  $\chi T$  in the thermodynamic limit [41]. However, the magnetic properties of studied compounds cannot be described by such a model even when interchain interaction is included in the mean-field approximation [42]. Another model was proposed accounting for an FM exchange interaction in dimeric Cu(II)-Mn(II) units, which are effectively coupled by AFM exchange interactions. An increase of  $\chi T$  of **4a** below 50 K is a clear indication of dominant FM exchange interaction and the influence of AFM exchange between dimers at low temperatures decreases slightly the value of  $\chi T$ . On the other hand, the influence of the AFM exchange interaction in **2** is much more pronounced yielding a significant decrease of  $\chi T$  at low temperature (an in-

crease of  $\chi T$  due to the FM intradimer interaction is suppressed) and to the presence of the LRO.

To confirm the presence of FM intradimer exchange interaction, the BS DFT calculations were performed using the X-ray-determined structural parameters of the molecule of **2** and **4a** to estimate the exchange interaction within the Cu(II)-Mn(II) dimers. The calculations employing PBE0 DFT functional yielded an FM exchange interaction  $J_{\text{BS}}/k_{\text{B}} = 1.14 \text{ K}$  and  $J_{\text{BS}}/k_{\text{B}} = 1.07 \text{ K}$  for compounds **2** and **4a**, respectively.

The experimental results were then analyzed using a model of the interacting  $S_{\text{Cu}}-S_{\text{Mn}}$  FM dimers using a spin Hamiltonian in the form  $\mathcal{H} = -J_{\text{Cu}}\hat{S}_{\text{Cu}}\hat{S}_{\text{Mn}}$  with the intradimer exchange interaction  $J$  ( $J = 2J_{\text{BS}}$ ) and including interdimer interaction  $zJ'$  in the mean-field approximation [40], where  $z$  is the number of nearest neighbors. A weak zero-field splitting typical for Mn(II) ions was neglected in the model. The fit was performed using a custom-made code in-

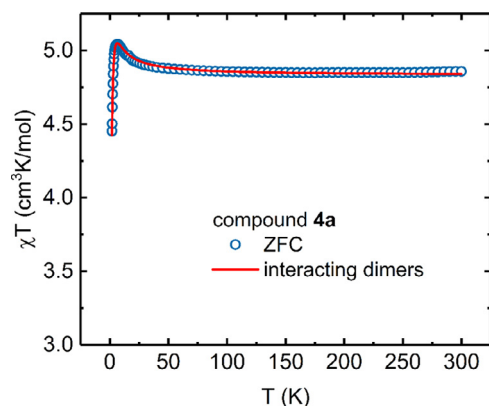
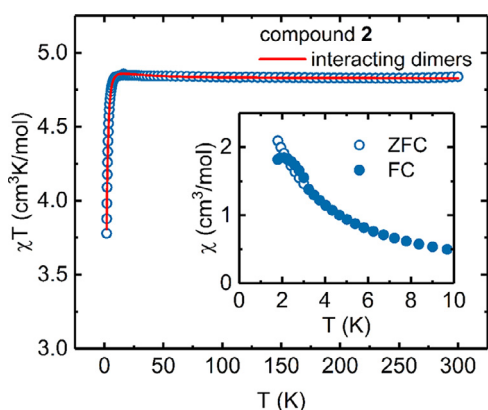


Fig. 10. Temperature dependence of the  $\chi T$  product of **4a** measured in ZFC regime (circles) and the fit of the interacting dimers model (solid line) with  $J/k_{\text{B}} = 2.34 \text{ K}$ ,  $zJ'/k_{\text{B}} = -0.042 \text{ K}$ ,  $g_{\text{Cu}} = 2.10$  and  $g_{\text{Mn}} = 2.01$ .



**Fig. 11.** Temperature dependence of the  $\chi T$  product of **2** measured in ZFC regime (circles) and the fit of the interacting dimers model (solid line) with  $J/k_B = 2.28$  K,  $zJ'/k_B = -0.065$  K,  $g_{Cu} = 2.09$ , and  $g_{Mn} = 2.01$ . Inset: Temperature dependence of the susceptibility of **2** measured in ZFC (open circles) and FC (full circles).

cluding the simulation package EasySpin [43]. The resulting values were  $J/k_B = 2.28$  K,  $zJ'/k_B = -0.065$  K,  $g_{Cu} = 2.09$ , and  $g_{Mn} = 2.01$  and  $J/k_B = 2.34$  K,  $zJ'/k_B = -0.042$  K,  $g_{Cu} = 2.10$  and  $g_{Mn} = 2.01$  for **2** and **4a**, respectively. This result confirms a sensitivity of the magnetic response on a subtle change of the interdimer interaction and very good agreement of the BS DFT calculations of intradimer exchange interaction with the experiment.

#### 4. Conclusion

Two organic ligands *dpc* and *dac* were prepared according to the synthetic procedure described by Royal et al. [14]. This procedure is strongly selective for the preparation of 1,8-trans disubstituted cyclams, runs at mild conditions, and leads to relatively high yields. We observed a lower yield in the case of preparation of *dpc*; therefore we lengthened the reaction time in the step of 1,8-Dipropyl-4,11-diazoniatriacyclo[9.3.1.14,8]hexadecane dibromide preparation. Using prepared ligands *dac* and *dpc*, Cu(II) complexes **1** and **3** with the analogous structure were prepared and consequently used for the synthesis of bimetallic complexes using the complex as ligand strategy, which should lead to the preparation of coordination compounds with predictable dimensionality. Thus, heterobimetallic compounds **2,4a**, and **4b** were prepared with analogous  $\{Cu(L)MnCl_4\}$  structure motif in each case. According to our knowledge, -Cu-Cl-Mn- structure motif in bimetallic complexes is rare. In the case of chain compound, it was observed previously only by  $Cu(en)_2MnCl_4$ , published by Chiari et al. [30], but similar systems based on *cyclam* or its derivatives and  $MnCl_4$  have not been registered in CCDC yet.

Bond distances characterizing coordination polyhedrons of Mn(II) and equatorial plane of Cu(II) are consistent with bond distances in already known complexes with analogous structure motif [30] as well as with complexes with ethane-1,2-diamine derivatives prepared by our research group. The difference occurs in the case of the Cu(II) coordination environment. In the case of ethane-1,2-diamine and its derivatives Cu(II) has tetragonal bipyramidal polyhedron and both axial distances have values near to the sum of VdW radii (2.804 and 3.063 in Chiari et al. [30]; 2.8714(15), 2.9426(7)–2.9706 in Samořová, private commns.). In complexes presented here, we observed the formation of binuclear complexes and the formation of chains connected through hydrogen bonds where the nearest Cu-Cl distance (Cu and Cl atoms are from different complex molecules) is longer than 3.5 Å.

In comparison to compounds with analogous crystal structures with ethylenediamine, a different system of hydrogen bonds is

present, and thus the formation of a 1D system is observed instead of 3D as published elsewhere (Samořová, private commns).

The magnetic properties of compounds **2** and **4a** are governed by the presence of an FM exchange interaction in bimetallic Cu(II)-Mn(II) units, which was confirmed by single-point BS DFT calculations.

#### Supplementary data

CCDC 2038711, 2038712, 2038713, 2038714 and 2038715 contain the supplementary crystallographic data for **1,3,2,4a** and **4b**, respectively. These data can be obtained free of charge via <http://www.ccdc.cam.ac.uk/conts/retrieving.html> (or from the Cambridge Crystallographic Data Centre, 12, Union Road, Cambridge CB2 1EZ, UK; fax: +44 1223 336033).

#### Declaration of Competing Interest

All of the authors have actively contributed to the experimental work, evaluation of the experimental results and preparation of the manuscript. The authors have no conflicts of interest to declare. All authors have read the manuscript and approve its submission.

#### CRediT authorship contribution statement

**Erika Samořová:** Investigation, Writing - original draft, Writing - review & editing. **Juraj Kuchár:** Conceptualization, Formal analysis, Resources, Supervision, Visualization, Writing - original draft, Writing - review & editing. **Erik Čiřmár:** Investigation, Visualization, Writing - original draft, Writing - review & editing. **Michal Dušek:** Data curation, Formal analysis.

#### Acknowledgments

The financial support for this work was given by the Slovak Research and Development Agency (APVV-18-0197 and APVV-18-0016) and the Scientific Grant Agency of Ministry of Education, Science, Research and Sport of the Slovak Republic (VEGA 1/0063/17, VEGA 1/0426/19) is acknowledged. CzechNanoLab project LM2018110 funded by MEYS CR is gratefullyacknowledged for the financial support of the measurements/samplefabrication at LNSM Research Infrastructure. This publication is the result of the project implementation: New unconventional magnetic materials for applications, ITMS 313011T544, supported by the Operational Programme Integrated Infrastructure 2014 - 2020 (OPII) funded by the ERDF. The authors are very grateful to Assoc. Prof. Ivan Potočňák, PhD. for measuring elemental analysis. E.S. thanks to the research group of Coordination and Bioinorganic Chemistry at Charles University in Prague for the opportunity to work in their laboratory.

#### Supplementary materials

Supplementary material associated with this article can be found, in the online version, at doi:[10.1016/j.molstruc.2021.130592](https://doi.org/10.1016/j.molstruc.2021.130592).

#### References

- [1] A.M. Tishin, Y.I. Spichkin, *The Magnetocaloric Effect and its Applications*, CRC Press, Boca Raton, 2016.
- [2] M. Verdaguer, A.N. Gleizes, *Magnetism: molecules to build solids*, Eur. J. Inorg. Chem. 9 (2020) 723–731.
- [3] E. Coronado, *Molecular magnetism: from chemical design to spin control in molecules, materials and devices*, Nat. Rev. Mater. 5 (2020) 87–104.
- [4] A.S. Boyarchenkov, I.G. Bostrem, A.S. Ovchinnikov, *Quantum magnetization plateau and sign change of the magnetocaloric effect in a ferrimagnetic spin chain*, Phys. Rev. 76 (2007) 224410–224418.

- [5] P. Konieczny, R. Peřka, D. Czernia, R. Podgajny, Rotating Magnetocaloric effect in an anisotropic two-dimensional  $\text{Cu}[\text{WV}(\text{CN})_8]_3^-$  molecular magnet with topological phase transition: experiment and theory, *Inorg. Chem.* 56 (2017) 11971–11980.
- [6] Y. Pei, M. Verdaguer, O. Kahn, J. Sletten, J.P. Renard, Magnetism of manganese(II)copper(II) and nickel(II)copper(II) ordered bimetallic chains. Crystal structure of  $\text{MnCu}(\text{pba})(\text{H}_2\text{O})_3 \cdot 2\text{H}_2\text{O}$  (pba = 1,3-propylenebis(oxamato)), *Inorg. Chem.* 26 (1987) 138–143.
- [7] O. Kahn, Y. Pei, M. Verdaguer, J.P. Renard, J. Sletten, Magnetic ordering of manganese(II) copper(II) bimetallic chains; design of a molecular based ferromagnet, *J. Am. Chem. Soc.* 110 (1988) 782–789.
- [8] R.D. Willett, D. Wang, Investigation of  $\text{Cu}(\text{macrocycle})\text{MX}_4$  magnetic chains, *J. Appl. Phys.* 73 (1993) 5384–5385.
- [9] L. Cui, J.Y. Ge, C.F. Leong, D.M. D'Allessandro, J.L. Zuo, A heterometallic ferrimagnet based on a new TTF-bis(oxamato) ligand, *Dalton Trans.* 46 (2017) 3980–3988.
- [10] J. Ferrando-Soria, D. Cangussu, M. Eslava, Y. Journaux, R. Lescouřezec, M. Julve, F. Lloret, J. Pasán, C. Ruiz-Pérez, E. Lhotel, C. Paulsen, E. Pardo, Rational enantioselective design of chiral heterobimetallic single-chain magnets: synthesis, crystal structures and magnetic properties of oxamato-bridged  $\text{M}(\text{II})\text{Cu}(\text{II})$  chains ( $\text{M}=\text{Mn}, \text{Co}$ ), *Chem. Eur. J.* 17 (2011) 12482–12494.
- [11] S. Yamamoto, T. Fukui, Thermodynamic properties of heisenberg ferrimagnetic spin chains: ferromagnetic-antiferromagnetic crossover, *Phys. Rev. B* 57 (1998) R14008–R14011.
- [12] J. Streřka, T. Verkholyak, Magnetic signatures of quantum critical points of the ferrimagnetic mixed spin-(1/2, S) heisenberg chains at finite temperatures, *J. Low Temp. Phys.* 187 (2017) 712–718.
- [13] G.A. Bain, J.F. Berry, Diamagnetic corrections and pascal's constants, *J. Chem. Educ.* 85 (2008) 532–536.
- [14] G. Royal, V. Dahaoui-Gindre, S. Dahaoui, A. Tabard, R. Guillard, P. Pullumbi, P. Lecomte, New synthesis of trans-disubstituted cyclam macrocycles-elucidation of the disubstitution mechanism on the basis of X-ray data and molecular modeling, *Eur. J. Org. Chem.* 9 (1998) 1971–1976.
- [15] Rigaku Oxford Diffraction CrysAlisPRO 1.171.39.35c, Rigaku Oxford Diffraction, Yarnton, England, 2017.
- [16] L. Palatinus, G. Chapuis, SUPERFLIP-a computer program for the solution of crystal structures by charge flipping in arbitrary dimensions, *J. Appl. Cryst.* 40 (2007) 786–790.
- [17] V. Petřicek, M. Dusek, L. Palatinus, Crystallographic computing system JANA2006: general features, *Z. Krist.* 229 (2014) 345–352.
- [18] K. Brandenburg, DIAMOND Version 4.5.1., Bonn, Germany, 2018.
- [19] R.C. Clark, J.S. Reid, The analytical calculation of absorption in multifaceted crystals, *Acta Cryst.* (1995) 887–897 A51.
- [20] H. Nagao, M. Nishino, Y. Shigeta, T. Soda, Y. Kitagawa, T. Onishi, Y. Yoshioka, K. Yamaguchi, Theoretical studies on effective spin interactions, spin alignments and macroscopic spin tunneling in polynuclear manganese and related complexes and their mesoscopic clusters *Coord. Chem. Rev.* 198 (2000) 265–295.
- [21] F. Neese, Software update: the ORCA program system, version 4.0, *WIREs Comput. Mol. Sci.* 8 (2017) e1327–e1333.
- [22] C. Adamo, V. Barone, Toward reliable density functional methods without adjustable parameters: the PBE0 model, *J. Chem. Phys.* 110 (1999) 6158–6170.
- [23] E. van Lenthe, E.J. Baerends, J.G. Snijders, Relativistic total energy using regular approximations, *J. Chem. Phys.* 99 (1994) 4597–4610.
- [24] C.J. van Wüllen, Molecular density functional calculations in the regular relativistic approximation: method, application to coinage metal diatomics, hydrides, fluorides and chlorides, and comparison with first-order relativistic calculations, *J. Chem. Phys.* 109 (1998) 392–399.
- [25] F. Weigend, R. Ahlrichs, Balanced basis sets of split valence, triple zeta valence and quadruple zeta valence quality for H to Rn: design and assessment of accuracy, *Phys. Chem. Chem. Phys.* 7 (2005) 3297–3305.
- [26] F. Neese, F. Wennmohs, A. Hansen, U. Becker, Efficient, approximate and parallel hartree-fock and hybrid DFT calculations. A 'chain-of-spheres' algorithm for the hartree-fock exchange, *Chem. Phys.* 356 (2009) 98–109.
- [27] F. Weigend, Accurate coulomb-fitting basis sets for H to Rn, *Phys. Chem. Chem. Phys.* 8 (2006) 1057–1065.
- [28] A. Hellweg, C. Hattig, S. Hofener, W. Klopper, Optimized accurate auxiliary basis sets for RI-MP2 and RI-CC2 calculations for the atoms Rb to Rn, *Theor. Chem. Acc.* 117 (2007) 587–597.
- [29] K. Yamaguchi, Y. Takahara, T. Fueno, Ab-initio molecular orbital studies of structure and reactivity of transition metal-OXO compounds, *Appl. Quantum Chem.* (1986) 155–184.
- [30] B. Chiari, A. Cinti, O. Piovesana, P.F. Zanazzi, Exchange interactions in the bimetallic chain compound  $\text{Cu}(\text{ethylenediamine})_2\text{MnCl}_4$ , *Inorg. Chem.* 34 (1995) 2652–2657.
- [31] N. Abdullah, Z. Arifin, E.R.T. Tiekink, N. Sharmin, N.S.A. Tajidi, S.A.M. Hussin, Complexes of nickel(II) carboxylates with pyridine and cyclam: crystal structures, mesomorphisms, and thermoelectrical properties, *J. Coord. Chem.* 69 (2016) 862–878.
- [32] P.V. Bernhardt, L.A. Jones, P.C. Sharpe, Nitrogen- and carbon-based isomerism in the copper(II) complexes of 6,13-dimethyl-1,4,8,11-tetraazacyclotetradecane-6,13-diamine, *J. Chem. Soc. Dalton Trans.* 0 (1997) 1169–1176.
- [33] L.G. Alves, M. Souto, F. Madeira, P. Adao, R.F. Munhá, A.M. Martins, Syntheses and solid state structures of cyclam-based copper and zinc compounds, *J. Organomet. Chem.* 760 (2014) 130–137.
- [34] S.L. Hart, R.I. Haines, A.B. Deeken, D. Wagner, Isolation of the trans-I and trans-II isomers of  $\text{Cu}(\text{II})$ (cyclam) via complexation with the macrocyclic host cucurbit[8]uril, *Inorg. Chim. Acta.* 362 (2009) 4145–4151.
- [35] T. Steiner, The hydrogen bond in the solid state, *Angew. Chem. Int. Ed.* 41 (2002) 48–76.
- [36] J. Bernstein, R.E. Davis, Graph set analysis of hydrogen bond motifs. , In: J.A.K. Howard, F.H. Allen, G.P. Shields (eds), *Implications of Molecular and Materials Structure for New Technologies*. NATO Science Series (Series E: Applied Sciences). 360. Springer, Dordrecht (1999)
- [37] T.H. Lu, S.C. Lin, H. Aneetha, K. Panneerselvam, C.S. Chung, Copper(II) complexes of C-meso-1,5,8,12-tetramethyl-1,4,8,11-tetraazacyclotetradecane: syntheses, structures and properties, *J. Chem. Soc. Dalton Trans.* 0 (1999) 3385–3391.
- [38] P.V. Bernhardt, N-methylation of diamino-substituted macrocyclic complexes: intermolecular reactions, *J. Chem. Soc. Dalton Trans.* 0 (1996) 4319–4324.
- [39] K.Y. Choi, J.C. Kim, W.P. Jensen, I.H. Suh, S.S. Choi, Copper(II) and Nickel(II) Complexes with 3,14-Di-methyl-2,6,13,17-tetra-azatri-cyclo[16.4.0.07,12]do-cosane,  $[\text{M}(\text{C}_{20}\text{H}_{40}\text{N}_4)]\text{Cl}_2 \cdot 2\text{H}_2\text{O}$  ( $\text{M} = \text{Cu}$  and  $\text{Ni}$ ), *Acta Cryst. C52* (1996) 2166–2168.
- [40] H. Čenčariková, J. Streřka, Unconventional strengthening of the bipartite entanglement of a mixed spin-(1/2,1) heisenberg dimer achieved through zeeman splitting, *Phys. Rev. B* 102 (2020) 184419.
- [41] K. Nakatani, J.Y. Carriat, Y. Journaux, O. Kahn, F. Lloret, J.P. Renard, Y. Pei, J. Sletten, M. Verdaguer, Chemistry and physics of the novel molecular-based compound exhibiting a spontaneous magnetization below  $T_c = 14$  K,  $\text{MnCu}(\text{obbz})\text{.cntdot.1H}_2\text{O}$  (obbz = oxamidobis(benzoato)). Comparison with the antiferromagnet  $\text{MnCu}(\text{obbz})\text{.cntdot.5H}_2\text{O}$ . Crystal structure and magnetic properties of  $\text{NiCu}(\text{obbz})\text{.cntdot.6H}_2\text{O}$ , *J. Am. Chem. Soc.* 111 (1989) 5739–5748.
- [42] C.J. O'Connor, Magnetochemistry-advances in theory and experimentation, *Prog. Inorg. Chem.* 29 (1982) 203–283.
- [43] S. Stoll, A. Schweiger, EasySpin, a comprehensive software package for spectral simulation and analysis in EPR, *J. Magn. Reson.* 178 (2006) 42–55.